8

This chapter is left somewhat unfinished. The higher-order Stokes phenomena (HOSP) is not so important until some of the more complex Stokes line problems in later chapters.

`Draft chapter last generated 2024-12-02; P.H. Trinh`

In the previous few chapters, we encountered the situation whereby a base asymptotic approximation switches on an exponentially-small term across Stokes lines. In the case of the exponential integral, this was a base series of phase zero; thus the asymptotic expansion for $y \sim y_0$ in (6.2) switches on $e^{-\chi/\epsilon}$ in the limit $\epsilon \to 0$. In the case of the second-order Airy equation, this was $e^{-2/3x^{3/2}}$ switching on $e^{2/3x^{3/2}}$ in the limit $|x| \to \infty$ as in (7.18). Both of these cases involve only a switching between pairs of asymptotic expansions. However, higher-order problems allow for the possibility of more than two exponential interactions, and this produces a curious issue.

Consider, for example, a problem where three exponentials are present, say $e^{-\chi_1/\epsilon}$, $e^{-\chi_2/\epsilon}$, and $e^{-\chi_3/\epsilon}$, with the singulant functions, χ_i considered to be functions of $z \in \mathbb{C}$. In the z-plane, consider the situation that occurs if the Stokes lines cross in the following configuration:

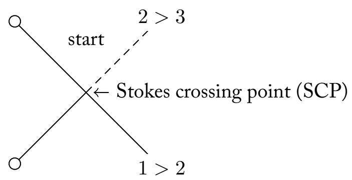

Figure 8.1

Begin at the point marked 'start' and let us assume that in this region the solution is approximated by $e^{-\chi_1/\epsilon}$. If we analytically continue anti-clockwise in a circle, we see the following transitions:

$$
\begin{aligned}
A_1 e^{-\chi_1/\epsilon} &\xrightarrow{1>2} A_1 e^{-\chi_1/\epsilon} + A_{12} e^{-\chi_2/\epsilon}, \\
&\xrightarrow{2>3} A_1 e^{-\chi_1/\epsilon} + A_{12} e^{-\chi_2/\epsilon} + A_{23} e^{-\chi_3/\epsilon}, \\
&\xrightarrow{1>2} A_1 e^{-\chi_1/\epsilon} + A_{23} e^{-\chi_3/\epsilon}, \\
&\xrightarrow{2>3} A_1 e^{-\chi_1/\epsilon} + A_{23} e^{-\chi_3/\epsilon} \quad \text{(same as above; } \chi_2 \text{ not present).}
\end{aligned}
$$

where all the prefactors are regarded as functions of z. Thus, by the time we return to the start point, both exponentials $e^{-\chi_1/\epsilon}$ and $e^{-\chi_3/\epsilon}$ are present and there is an inconsistency. Note that we have drawn a section of the $2 > 3$ Stokes line as dashed as it is an *irrelevant Stokes line*—there is no switching since the exponential $e^{-\chi_2/\epsilon}$ is not present.

irrelevant Stokes line

However, for a different choice of start point or starting exponential, this line may be relevant.

At this point, there are two possibilities that seem plausible: (i) there is an additional Stokes line unaccounted for that might, for instance, switch off the $e^{-\chi_3/\epsilon}$ contribution; or (ii) one of the illustrated Stokes lines should not be be there. This thought experiment illustrates the fact that, when two Stokes lines cross at the Stokes crossing point (SCP), with the two Stokes lines possessing a shared exponential, there may be additional subtleties that result.

In fact, the answer that occurs in certain situations is a combination of the two items above. Let us propose that there is, in fact, an unaccounted singularity that generates a missing $1 > 3$ Stokes line; this missing Stokes line must travel through the intersection point in order to resolve the inconsistency. For example, we might propose:

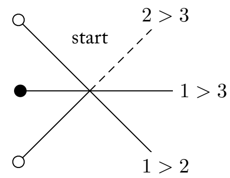

Figure 8.2

This configuration does not work, either, because in general whatever is switched on across one section of $1 > 3$ is switched off by the other, and the original issue of an orphaned exponential $A_{23}e^{-\chi_3/\epsilon}$ remains.

Instead, in this chapter, we demonstrate an example where the unusual alternative configuration occurs:

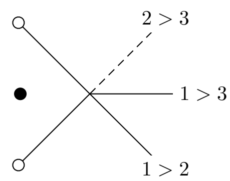

Figure 8.3

Therefore, the $1 > 3$ Stokes line, in fact, disappears along one of its sections! This unusual situation, where the activity of a Stokes line changes across a Stokes crossing point is associated with the *higher-order Stokes Phenomenon.* We say that a portion of the $1 > 3$ line is *inactive*. In this chapter, we shall make this phenomenon transparent by a steepest descent analysis of a toy problem.

inactive Stokes line

Before presenting this, it sufficient for us to provide a hint of the reason why such a situation can occur. Consider a steepest descent analysis of an integral of the form

$$I(z) = \int_C e^{-\chi(s;\,z)/\epsilon}\, ds,$$

in the limit $\epsilon \to 0$, and where there are three saddle points in the complex s-plane, say at $s = s_1, s_2, s_3$. At a particular value of the parameter $z = z^*$, it can be the case that

$$\text{Im}[\chi(s_1; z^*) - \chi(s_3; z^*)] = 0, \qquad \text{Re}[\chi(s_1; z^*) - \chi(s_3; z^*)] \geq 0.$$

Normally, this would indicate that z^* lies on a Stokes line in the z-plane, and there exists a path of steepest descent between saddle points s_1 and s_3; here, the saddle-point contribution from s_1 is expected to switched-on the contribution from s_3. However, this local condition is not sufficient to guarantee such a path—and indeed there may be no such path depending on the global configuration of the χ function in the s-plane. This is essentially the issue—the local Stokes line criterion fails because the integration topology is more complicated.

8.1 THE PEARCEY INTEGRAL

This presentation uses an integral related to the Pearcey function in order to illustrate the higher-order Stokes Phenomenon, and follows a development shown in Howls et al. [2004]. The Pearcey function forms one of the canonical functions of catastrophe theory (and one of the first seven catastrophe geometries, cf. Poston and Stewart [2014]) and arose in Pearcey's investigation of electromagnetic fields near a cusp [Pearcey, 1946]. More details can be found in the investigations of Connor and Curtis [1982], Connor et al. [1983] to investigate the numerical approximations.

Consider the integral with $\epsilon > 0$,

$$I(z) = \int_C \mathrm{e}^{-f(s;\, z)/\epsilon}\, \mathrm{d}s, \tag{8.1}$$

with

$$f(s;\, z) = -\mathrm{i}\left(\frac{1}{4}s^4 + \frac{1}{2}s^2 + sz\right). \tag{8.2}$$

The contour C is defined as a contour that starts at $\infty \exp(-\frac{3}{8}\pi \mathrm{i})$ and ends at $\infty \exp(\frac{1}{8}\pi \mathrm{i})$. The parameter in (8.2) is defined to be complex-valued, $z \in \mathbb{C}$.

Our plan is to apply the method of steepest descents and seek a deformation of C and subsequent asymptotic expansion of the integral in the limit $\epsilon \to 0$. There are three saddle points, located at $f'(s) = 0$, and we shall define the saddle points as

$$s = s_n(z), \qquad \text{where } s_n^3 + s_n + z = 0, \qquad n = 0, 1, 2. \tag{8.3}$$

Note that when $z = 0$, the saddle points lie at $s_0 = -\mathrm{i}$, $s_1 = 0$, and $s_2 = \mathrm{i}$. For other values of z, we shall index the three saddle points so that they are a smooth analytic continuation of these values at $z = 0$.

Note that we can write re-write (8.2) as

$$f(z) = \frac{1}{4} z f'(z) - \frac{\mathrm{i}}{4} z(z + 3a), \tag{8.4}$$

so the height of the saddle points are given by

$$F_n(z) \equiv f(s_n;\, z) = -\frac{\mathrm{i}}{4} s_n(s_n + 3z) \quad \text{for } n = 0,\, 1,\, 2. \tag{8.5}$$

The paths of steepest descent that emerge from the saddle point at $s = s_n$ are given by an equal phase condition and furthermore, a condition that ensures that each point on the contour, $s \in C_n$, lies downhill from the height of the saddle point:

$$C_n = \{s \in \mathbb{C} : \mathrm{Im}[f(s) - f(s_n)] = 0,\ \mathrm{Re}[f(s) - f(s_n)] \geq 0\}, \quad n = 0, 1, 2.$$

An example of a path of steepest descent is shown in fig. 8.4 where the intial contour is deformed through the lower most saddle point, $s = s_0$ via curve C_0.

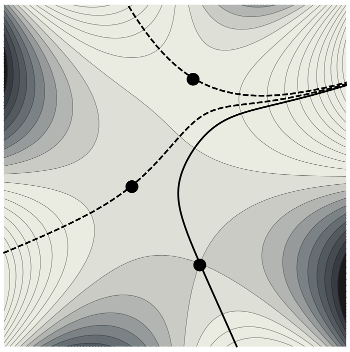

Figure 8.4: An example of the deformation through saddle point s_0 and via contour C_0. This shows the s-plane at the value of $z = 0.61 + 0.2\mathrm{i}$.

As the value of the parameter, z, varies in the complex z-plane, the saddle points will shift in the s-plane, and the set of relevant steepest descent contours that we must deform the original contour, C, into may change. We consider those special values of $z \in \mathbb{C}$, where the steepest descent contour through a saddle z_i passes through a neighbouring saddle, say z_j, and hence the curve C is then deformed to $C_i \cup C_j$. These characterise the Stokes lines in the z-plane, and are given by:

$$S_{i>j} = \{z \in \mathbb{C} : \mathrm{Im}[F_j(z) - F_i(z)] = 0 \text{ and } \mathrm{Re}[F_j(z) - F_i(z)] \geq 0\}, \tag{8.6}$$

where recall we have written $F_j(z) = f(s_j, z)$ to emphasise the dependence on z. Notice in the above condition that the height at the saddle z_j, or more precisely the magnitude of the integrand, is characterised by $\exp[-\mathrm{Re}(F_j)/\epsilon]$. This magnitude is exponentially smaller than the corresponding magnitude from saddle z_i, characterised by $\exp[-\mathrm{Re}(F_i)/\epsilon]$. Thus the j^{th} saddle lies downhill of the i^{th} saddle and consequently, we say that the exponential corresponding to the i^{th} saddle switches-on the exponential corresponding to the j^{th} saddle across the Stokes line $S_{i>j}$ in the z-plane.

In the z-plane, the Stokes lines originate from where $F_i(z) = F_j(z)$, and these critical points can be found as follows. First, two critical points are characterised by points where two of the three saddles are associated with a double root of the cubic equation. Here, $s_n = \pm\mathrm{i}/\sqrt{3}$ and substitution into $f(s_n;\, z) = 0$ yields

$$z_{\pm} = \pm\left(\frac{4}{27}\right)^{1/2}\mathrm{i}. \tag{8.7}$$

It can be verified that the positive sign corresponds to where $F_0(z_+) = F_1(z_+)$ and the negative sign to $F_1(z_-) = F_2(z_-)$. The last critical point is verified to be at $z = 0$ and here $F_0(0) = F_2(0)$.

We now plot the three critical points and their associated Stokes lines from condition (8.6), and this is shown in fig. 8.5. We see from the diagram that, like the conceptual picture illustrated in fig. 8.2 there is a Stokes crossing point (SCP). We consider the different contributing exponentials that result when the parameter z is analytically continued along the dashed path encircling the SCP. At the beginning of this path, we assume that the solution is approximated by integration along C_0, as in fig. 8.4. So we write this conceptually as

$$I(z) = \mathcal{O}(\mathrm{e}^{-F_0/\epsilon}) \sim ⓪ .$$

Next, as we analytically continue along the indicated path, we observe that by the time the end of the path is reached, we have ⓪ and ② . *There is an inconsistency.* One sensibly concludes that either the set of Stokes lines is incomplete, and there are additional Stokes lines present that are unaccounted for, or some of the the previously predicted Stokes lines are incorrect. The case turns out to be the latter, and in fact, the solid blue line that lies to the left of the triple intersection point is an inactive Stokes line. We now examine this more closely via the steepest descent analysis.

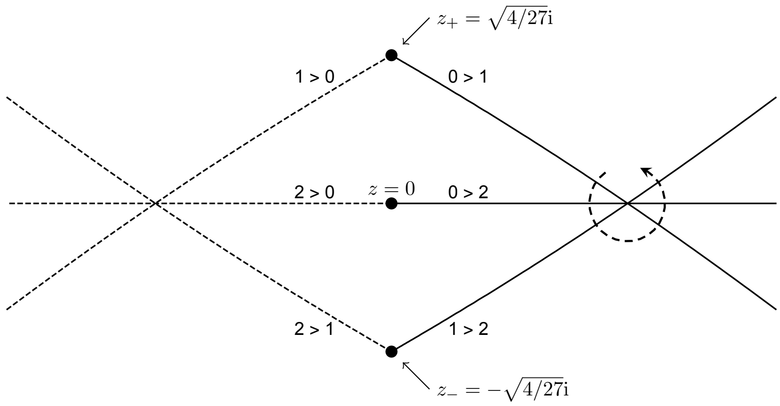

Figure 8.5: Stokes lines in the z-plane. We consider the $\mathrm{Re}(z) > 0$ region, where the switchings are all denoted with solid lines. We analytically continue along the curved dashed line beginning with ⓪ and by the time the end of the arrow is reached, ⓪ and ② , are expected to be present, yielding an inconsistency.

8.2 A CLOSER LOOK AT THE STEEPEST DESCENT CURVES

We take a circular path around the Stokes crossing point, as shown in fig. 8.6. The steepest descent contours in the s-plane are shown for specific points. Observations include:

(a) Starting from the top, we have only the '0' exponential.
(b–c) As we cross the $0 > 1$ line, we turn on the '1' exponential.
(d) However, at the line that was anticipated to be $0 > 2$, no switching occurs since 2 is not adjacent to 1. We call the $0 > 2$ line here *inactive*.
(e–f) We cross the $1 > 2$ line and switching occurs.
(g–h) Again, $0 > 1$ switching occurs, and now we only have $0, 2$ present.
(i) This time the $0 > 2$ line is active. We can see that 0 is adjacent to 2 and now 2 is switched off.
(j) There is supposed to be a $1 > 2$ Stokes line here. There is in the sense that, had 1 been present, it would switch on/off 2. However, in this case, the Stokes line is *irrelevant*.

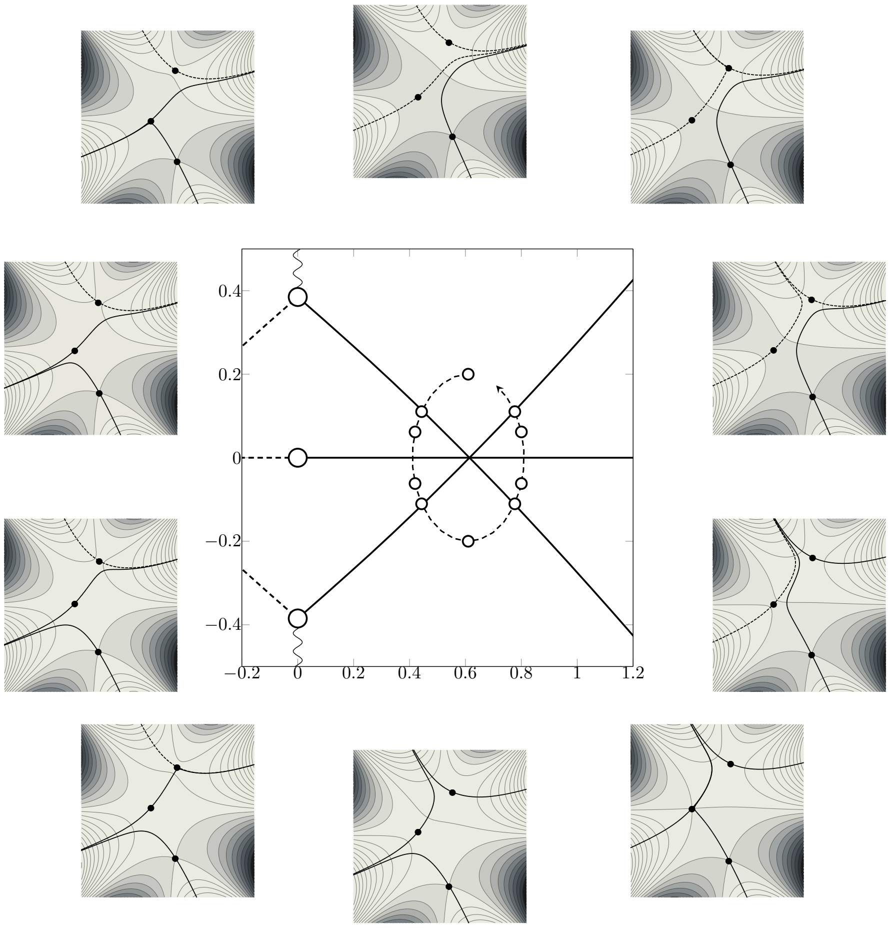

Figure 8.6: The z-plane is shown centre, with the SCP lying at approximately $a \approx 0.61$. The analytically continue in a circular route around the SCP. The insets displayed around the central picture show the steepest descent curves in the s-plane.

8.3 INTERPRETATION IN THE BOREL PLANE

Like for the analysis of the Airy equation in **??**, it is possible to perform a transformation from the original integration plane (the s-plane) to the Borel plane (the u-plane) via $u = f(s;\, z)$. This allows us to visualise the switching of exponentials from within the u-plane, where the steepest descent paths are much simpler and lie along $\operatorname{Im} u = \text{const.}$ However, the complexity in the integration problem now appears in the multi-valued structure of the integrand.

In this case, let us define u via

$$u = f(s;\, z) \equiv -\mathrm{i}\left(\frac{1}{4}s^4 + \frac{1}{2}s^2 + sz\right). \tag{8.8}$$

When we invert the above quartic equation and obtain values of s given values of u, we obtain four branches. Thus, let us write

$$s \equiv G_i(u;\, z) = f^{-1}(u;\, z), \tag{8.9}$$

where $G = G_i$, $i = 1, \ldots 4$ prescribes the four branches. Thus u is said to lie on a Riemann surface with four Riemann sheets. The integral (8.1) now becomes

$$I(z) = \int_{C_u} G_i'(u;\, z)\mathrm{e}^{-u/\epsilon}\, \mathrm{d}u = \int_{C_u} \left[\frac{1}{f'(s = G_i(u; z); z)}\right] \mathrm{e}^{-u}\, \mathrm{d}u. \tag{8.10}$$

Note from the above form that the three saddle points in the s-plane, where $f' = 0$, correspond to singularities in the integrand function in the u-plane. There are thus three square-root branch points in the Borel plane, $u_i(z) = f(s_i; z)$ that relate the four Riemann sheets.

For a given curve of integration, C, of the original integral (8.1), we should consider its mapped image, C_u, which will lie on one of the four possible Riemann sheets. However, for the following, it is simpler to consider the choice of C_u consisting of a path of integration that runs from $u = \infty + a\mathrm{i}$, encircles a saddle point, and returns to $u = \infty + b\mathrm{i}$ for appropriately chosen a and b (which will be clear momentarily). This choice is accompanied by choosing one of the possible ($i \in \{1, 2, 3, 4\}$) Riemann sheets that prescribes G_i in the integrand.

8.3.1 A visualised example

The above can be made clear with an example. Let us take $z = 0.61+0.3\mathrm{i}$. There are three saddle points in the s-plane, $s = s_j$ for $j = 0, 1, 2$, found from (8.3), and these correspond to square-root branch points $u = u_j$. For the stated value of z, these are approximately given by

$$s_0 = 0.32 - 1.00\mathrm{i}, \quad s_1 = -0.52 - 0.17\mathrm{i}, \quad s_2 = 0.20 + 1.17\mathrm{i}$$
$$u_0 = -0.55 - 0.15\mathrm{i}, \quad u_1 = -0.15 + 0.14\mathrm{i}, \quad u_2 = 0.70 + 0.51\mathrm{i}$$

With s_0 chosen to be the saddle point in the lower right, we now design a rectangular contour C_u, that encircles the point, u_0, and that lies on one of the four Riemann sheets. We shall designate this as the 'central' Riemann sheet and in the visualisations shown below, this corresponds to the choice of $s = G_2(u; z)$—note though that this is a function of our relatively arbitrary labelling scheme for the Riemann sheets.

In fig. 8.7 we show the central Riemann sheet. The rectangular C_u contour of integration is shown bolded. The branch point u_0 is shown with the white circle. The light gray contours correspond to $\mathrm{Re}(s) = \mathrm{Re}(G_2(u))$. The branch cut from $u = u_0$ is the thick black line taken to the right. The cut structure of the light gray contours show a discontinuity in $G_2(u)$, as expected, across the cut. Note that in order to construct this plot, we must invert the function (8.8) in a manner consistent with the desired branch structure—its computation is non-trivial.

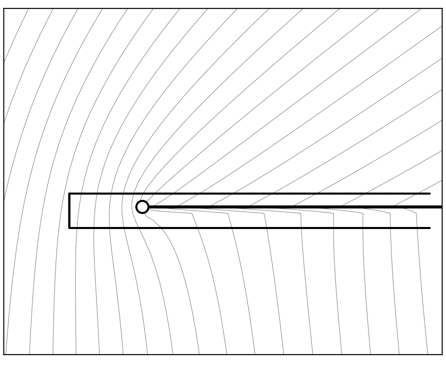

Figure 8.7: $z = 0.61 + 0.3\exp(\pi i/2)$. The central Riemann sheet, $G_2(u)$ is shown. There is only a single branch point here, with $u = u_0$. The contour C_u starts from ∞, loops around u_0, and returns to ∞.

Next, in fig. 8.7, we show the original integration s-plane, with the images of C_u. The three saddle points, s_0, s_1, s_2 are shown as circles, and the steepest descent trajectories through these points are marked C_1, C_2, and C_3. There are, in fact, four images of C_u found via $s = G_i(C_u)$. The contour in the lower right is precisely the one that corresponds to the $i = 2$ Riemann sheet, $G_2(C_u)$.

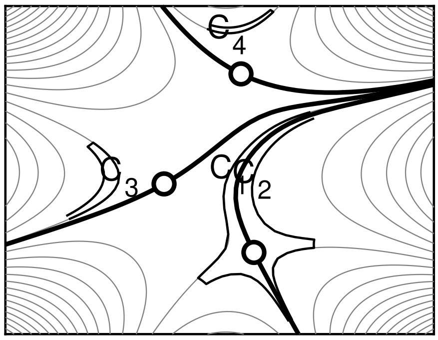

Figure 8.8: $z = 0.61 + 0.3\exp(\pi i/2)$. The central Riemann sheet, $G_2(u)$ is shown left. There is only a single branch point here, with $u = u_0$. The s-plane is shown right, with the four images of C_u drawn.

Thus in the u-plane of fig. 8.7, we note that the steepest descent deformation of C_u consists of the two horizontal line segments:

$$C_u^{(1)} = \{w + \mathrm{i}\,\mathrm{Im}(u_0)^+,\ w = \infty \ldots \mathrm{Re}(u_0)\}$$
$$C_u^{(2)} = \{w + \mathrm{i}\,\mathrm{Im}(u_0)^-,\ w = \mathrm{Re}(u_0) \ldots \infty\}.$$

In the s-plane, this corresponds to the choice of steepest descent contour through s_0, marked with C_2 in fig. 8.8.

A better visualisation of the relationships between the Riemann sheets is shown in the right illustration of **??**. There are four planes corresponding to the four Riemann sheets, G_i. The white circles correspond to the three branch points $\{u_0, u_1, u_2\}$. From each brach point, there is a solid line showing the branch cut, and we have used vertical lines to indicate how the Riemann sheets are connected. For instance, analytic continuation across the branch cut from u_0 on sheet G_2 proceeds to sheet G_1. Notice another key point, which is that not all three branch points are present on a given Riemann sheet.

8.4 JUSTIFICATION BY THE METHOD OF TERMINANTS

NB: My understanding of this is pretty tenuous. Primary source appears to be from Berry and Howls [1991], which was used as the basis of Howls et al. [2004], itself based on Langman [2005]. These techniques seem to go back to Howls' PhD thesis (no copy available) and then before that Dingle [1973].

Let us study an integral about a saddle point, $z = z_n$, written as

$$I^{(n)}(k) = \int_{C_n(\theta_k)} \mathrm{d}z\, g(z)\mathrm{e}^{-kf(z)}, \tag{8.11}$$

studied in the limit $k \to \infty$. Above, we assume that C_n has been deformed to the path of steepest descent through the saddle point at $z = z_n$, where $f'(z) = 0$. Writing $f(z_n) = f_n$, then if $z \in C_n$, then

$$\mathrm{Re}[k(f(z) - f_n)] \geq 0.$$

We now introduce the notation of

$$I^{(n)}(k) = \frac{1}{\sqrt{k}}\mathrm{e}^{-kf_n}T^{(n)}(k), \tag{8.12a}$$

$$T^{(n)}(k) = \sqrt{k}\int_{C_n(\theta_k)} \mathrm{d}z\, g(z)\mathrm{e}^{-k[f(z)-f_n]}, \tag{8.12b}$$

which essentially serves to localise the integration around the saddle point.

The goal is to seek asymptotic expansions and their remainders in the limit $k \to \infty$. In most practical applications of the method of steepest descent that we have used so far, only the first term of the series is obtained. To develop higher-order terms, we use the (Borel) transformation of

$$u(z) \equiv k[f(z) - f_n].$$

Note that for each value of z on C_n, u is real and non-negative. Moreover, for each value of u, except at $u = 0$, there are two values of z. We assume that $z = z_n^-(u)$ for the curve entering the saddle point, where u runs from ∞ to 0; similarly $z = z_n^+(u)$ for the curve leaving the saddle point, with u running from 0 to ∞. Then changing to differentiation in u, we have

$$T^{(n)}(k) = \frac{1}{\sqrt{k}}\int_0^\infty \mathrm{d}u\, \mathrm{e}^{-u}\left\{\frac{g(z_+(u))}{f'(z_+(u))} - \frac{g(z_-(u))}{f'(z_-(u))}\right\}. \tag{8.13}$$

8.5 Analysis of the differential equation

Has this ever been done? It should be similar to Mortimer [2004], Chapman and Mortimer [2005], so you get the higher-order Stokes Phenomenon via an additional approximation of the remainder terms. Need to first convert Pearcey to an ODE though. Note that

$$\frac{\mathrm{d}}{\mathrm{d}z}\left(-\frac{f}{\epsilon}\right) = \frac{\mathrm{i}s}{\epsilon},$$

then we have that

$$I'''(z) = \int_C \left(\frac{\mathrm{i}s}{\epsilon}\right)^3 \mathrm{e}^{-f/\epsilon}\,\mathrm{d}s.$$

We can then write

$$-\frac{\mathrm{i}s^3}{\epsilon^3} = -\frac{\mathrm{i}}{\epsilon^3}\left(s^3 + s + z - s - z\right) = \frac{1}{\epsilon^3}f'(s) + \frac{\mathrm{i}}{\epsilon^3}(s + z),$$

and thus

$$I'''(z) = -\frac{1}{\epsilon^2}\int_C \frac{\mathrm{d}}{\mathrm{d}s}\left(\mathrm{e}^{-f/\epsilon}\right)\,\mathrm{d}s + \frac{\mathrm{i}}{\epsilon^3}\int_C (s+z)\mathrm{e}^{-f/\epsilon}\,\mathrm{d}s = \frac{1}{\epsilon^2}I' + \frac{\mathrm{i}}{\epsilon^3}zI,$$

so we have the differential equation

$$\epsilon^3 I'''(z) = \epsilon I'(z) + \mathrm{i}zI(z), \tag{8.14}$$

with appropriate boundary conditions so that the solution decays. Note that we can verify that (8.14) returns to the integral equation using Fourier transform in (7.8) and applying a similar procedure to the Airy equation.

We can then apply the same methodology as the Airy equation. Set $I(z) = A(z)\mathrm{e}^{S(z)/\epsilon}$, where we find that

$$(S')^3 = S' + z. \tag{8.15}$$

We then set $S = S_0(z)$ and seek the differential equation for $A(z)$ and then expand

$$A(z) = \sum \epsilon^n A_n(z). \tag{8.16}$$

We would then find the $0 > 1$ and $0 > 2$ possible switchings by examining the divergent series in A. Anyways, this would give us the standard Stokes line switchings. But how do we predict the higher-order Stokes Phenomenon? If it is analogous to Chapman and Mortimer [2005], then the divergence of the late terms A_n should involve a recurrence relation that needs to be estimated using WKB techniques.